

## Crossover from single-level to multilevel transport in artificial atoms

E. B. Foxman, U. Meirav, P. L. McEuen, M. A. Kastner, O. Klein, P. A. Belk, and D. M. Abusch

*Department of Physics and Research Laboratory of Electronics, Massachusetts Institute of Technology, Cambridge, Massachusetts 02139*

S. J. Wind

*IBM Thomas J. Watson Research Center, Yorktown Heights, New York 10598*

(Received 28 February 1994)

Measurements are reported of the temperature dependence of the conductance through a small region of electron gas separated from its leads by tunnel junctions. The quantization of charge and energy in the small region gives rise to sharp, nearly periodic peaks in the conductance as a function of electron density, one for each electron added to the isolated region. Because the charge and energy are quantized, we call this an artificial atom. At low temperature, the conductance is limited by resonant tunneling through a single quantum level of the artificial atom, but at high temperatures several levels participate. Changes in the temperature dependence of the width and height of conductance peaks display clear evidence for this crossover from single-level to multilevel transport.

### I. INTRODUCTION

When electrons are confined to a small particle of metal or a small region of semiconductor, both the energy and charge of the system are quantized. In this way such nanometer-sized systems behave like artificial atoms.<sup>1</sup> Structures in which electrons are confined in a semiconductor are often called quantum dots. The quantization of energy is familiar: the solutions of the Schrödinger equation in an isolated region have discrete energies. In some ways, however, the quantization of charge is more mysterious. We are quite comfortable with the idea that the charge of a collection of electrons is discrete. However, the charge in any small volume of a larger sample of conductor is *not* discrete because the electronic wave functions are extended over the entire sample. Only when the states are localized is the charge quantized.

There is an intimate connection between the quantization of energy and that of charge. Consider a one-dimensional potential consisting of two equal barriers. This is a good model for an artificial atom because its properties are invariably measured by studying the variations in tunneling rates of electrons onto the atom from its leads. For large barriers the energy spectrum for the region between the barriers is nearly discrete. In reality the spectrum is continuous because each level has a Lorentzian line shape resulting from the finite coupling to the continuum outside the barriers. However, the width of the Lorentzian  $\Gamma$  can be very narrow because it decreases exponentially with the height and width of the barrier. The condition for energy quantization is that  $\Gamma < \Delta E$ , where  $\Delta E$  is the typical spacing between levels. This is the same condition that Thouless<sup>2</sup> gives for localization of the electronic wave functions. It leads to the criterion for localization that the conductance  $G < e^2/h$ . This is, therefore, not only the condition for energy quantization, but also the condition for charge quantization. For  $\Gamma < \Delta E$  the wave functions have exponentially small amplitudes outside the confined region, so the

charge between the barriers is discrete. Thus even at zero temperature single-electron phenomena can be seen in mesoscopic systems only if  $G < e^2/h$ .

The charge quantization leads to the interaction energy  $U$  for adding or removing a single electron. For a metal particle  $U = e^2/2C$ , where  $C$  is the total geometrical capacitance between the particle and all other electrodes. This charging energy gives rise to the Coulomb blockade of current at low temperature.<sup>3</sup> For a metal particle, the charging energy is always the same, no matter how many electrons are added, because the excess charge resides near the surface of the particle. On the other hand, for electrons confined in a region of a semiconductor the added charge is distributed in a way that depends on the state in which the extra electron resides. Thus  $U$  varies with the number of added particles because it depends on the details of the electronic wave functions.<sup>4</sup> This is similar to the case of natural atoms, in which the ionization potential and electron affinity are sensitive to the state to which the electron is added or from which it is removed.

Thus, in addition to  $kT$ , there are three energy scales of importance:  $U$ ,  $\Delta E$ , and  $\Gamma$ .  $U$  is the typical energy for adding an extra electron, and  $\Delta E$  is the typical excitation energy of the artificial atom. For structures in which single-electron phenomena have been observed, the three energy scales have the following order:  $U > \Delta E > \Gamma$ . Since  $kT$  is usually larger than  $\Gamma$ , there are two interesting temperature regimes. One corresponds to  $U > kT > \Delta E > \Gamma$ , and we call this the multilevel regime because there are more than one level within  $kT$ . This is the regime in which the Coulomb blockade model works well.<sup>3</sup> It is the only regime that can be accessed for metal artificial atoms, because for metals  $\Delta E$  is always very small. However, for sufficiently small semiconductor structures one can reach the limit in which  $U > \Delta E > kT > \Gamma$ , so that the properties of single levels are evident.<sup>5,6</sup>

This single-level regime is very interesting. Because the confining potential is not highly symmetric, one expects the system to be an example of quantum chaos, and

several interesting predictions have been made.<sup>7-9</sup> For example, random matrix models can explain why the heights of conductance peaks resulting from resonant tunneling through individual levels are found to be random, and the distribution function of the peak conductance has been predicted.<sup>7,8</sup> However, to test these predictions one must prove that the conductance is dominated by a single level.

In this paper we present results of a detailed study of the temperature dependence of conductance peaks for an artificial atom in GaAs. We show clear evidence of the crossover from single-level to multilevel conductance. However, even in the single-level regime, levels that have small conductance are masked by others nearby in energy. Theoretical work<sup>10-12</sup> provides a framework for ascertaining when the properties of a given level can be measured.

The organization of this paper is as follows: In Sec. II we review the current theoretical understanding of artificial atoms. Section III gives a description of the device structure. In Sec. IV we present the results of our measurements and compare them with theory. Finally, in Sec. V we give our conclusions.

## II. THEORETICAL BACKGROUND

The single-electron transistor is one fascinating type of artificial atom. The device consists of a region in which electrons are confined, separated from the current-carrying leads by tunnel barriers. The chemical potential can be changed by means of a gate electrode. The conductance of the single-electron transistor as a function of the gate voltage consists of a series of sharp peaks. If the transistor is made of metal the peaks are equally spaced and have equal, temperature-independent, amplitudes. However, for the semiconductor structure of Meirav, Kastner, and Wind,<sup>13</sup> quantum-mechanical effects cause the positions in the gate voltage to vary a little, the amplitudes to vary a lot, and the temperature dependence to be peculiar.

The simple behavior of the metal transistors is explained by the Coulomb blockade model: There is a

Coulomb blockade gap for tunneling at all values of the gate voltage except for the special values for which the energy of the atom for  $N$  and  $N+1$  electrons is equal.

To explain the quantum-mechanical effects, Meir, Wingreen, and Lee,<sup>9</sup> Beenaker<sup>11</sup> and others developed the constant-interaction model. This assumes that  $U$  is fixed, as in the metal single-electron transistor, independent of the number of electrons added to it. The Coulomb blockade gap collapses at the charge degeneracy point as it does for the metal transistor. However, in semiconductor structures the spacing of levels for excitation within the artificial atom is large enough so that at low  $T$  only one level determines the conductance. McEuen *et al.* showed<sup>4</sup> that the constant-interaction model is too simple because  $U$  is not the same for every added electron. However, they showed that for a limited number of electrons added, the constant-interaction model works quite well. In addition, for the issues explored here, variations of  $U$  are probably unimportant. We therefore use the constant-interaction model to analyze our results.

For the single-level limit ( $U > \Delta E \gg kT$ ) and the multilevel limit ( $U > kT \gg \Delta E$ ), the conductance peaks are described by simple analytic expressions. Consider first the single-level regime: Beenaker<sup>1</sup> suggested that the form for resonant tunneling of noninteracting particles should describe this case even though Coulomb interactions are obviously important. At zero temperature this gives

$$G_s = p \frac{e^2}{h} \frac{\Gamma_L \Gamma_R}{(E - E_0)^2 + \Gamma^2}, \quad (1)$$

with  $E = \mu$  the chemical potential. Here  $\Gamma_L$  and  $\Gamma_R$  are the tunneling rates (multiplied by  $\hbar$ ) through the left and right barriers, respectively,  $\Gamma = (\Gamma_L + \Gamma_R)/2$ , and  $p$  is the level degeneracy. At finite temperature the conductance is given by the convolution of  $G(E)$  in Eq. (1) with the negative derivative of the Fermi-Dirac distribution function, so the conductance is given by

$$G_s = p \frac{e^2}{h} \frac{\Gamma_L \Gamma_R}{\Gamma^2} \int \frac{dE}{kT} \left\{ \frac{\Gamma^2}{(E - E_0)^2 + \Gamma^2} \right\} \text{sech}^2 \left( \frac{E - \mu}{2kT} \right). \quad (2)$$

Since the Lorentzian becomes a  $\delta$  function in the limit  $\Gamma \rightarrow 0$ ,  $G_s$  for narrow resonances is proportional to the derivative of the Fermi-Dirac function ( $\text{sech}^2[(E - \mu)/2kT]/kT$ ). In our experiments  $\mu$  is varied by changing the voltage  $V_g$  on a gate electrode near the artificial atom. In the limit  $\Gamma \ll kT$ , Eq. (2) reduces to

$$G_s = p \frac{e^2}{h} \pi \frac{\Gamma_L \Gamma_R}{\Gamma} \frac{kT}{2} \text{sech}^2 \left( \frac{E_0 - \alpha e V_g}{2kT} \right), \quad (3)$$

where we have used  $\mu = \alpha e V_g$ , and  $\alpha$  is measured as discussed below. Meirav, Kastner, and Wind<sup>13</sup> showed that

Eq. (2) is in excellent agreement with experimental shapes of conductance peaks.

In the multilevel regime, the conductance is given by Kulik and Shekhter:<sup>14</sup>

$$G_m = \frac{e^2}{h} \frac{\rho}{4} \frac{\Gamma_L \Gamma_R}{\Gamma} \frac{\mu_c - \alpha e V_g}{kT} \times \text{csch} \left( \frac{\mu_c - \alpha e V_g}{kT} \right), \quad (4)$$

where  $\rho$  is the density of levels ( $1/\Delta E$ ) and  $\mu_c$  is the chemical potential for which there is a charge degeneracy point for the artificial atom. That is,  $\mu_c/\alpha e$  is the gate

voltage at which the states with  $N$  and  $N+1$  electrons have the same energy, the condition for a conductance peak. To better than 1% Eq. (4) is equivalent to

$$G_m = \frac{e^2}{h} \frac{\rho}{4} \frac{\Gamma_L \Gamma_R}{\Gamma} \operatorname{sech}^2 \left[ \frac{\mu_c - \alpha e V_g}{2.5kT} \right]. \quad (5)$$

The shapes of the resonances for the two ( $U > kT > \Delta E > \Gamma$ ) regimes are thus indistinguishable. However, the temperature dependencies are different. The peak height for the single-level conductance is proportional to  $1/T$ , whereas for the multilevel conductance it is temperature independent. Furthermore, the full width at half maximum of the peak is  $3.5kT$  for the single-level case and  $4.35kT$  for the multilevel case. We show below that these predictions are confirmed by our experiments.

### III. DEVICE STRUCTURE AND EXPERIMENTAL DETAILS

The measurements reported here were made with GaAs layers grown by molecular-beam epitaxy (MBE) on  $\text{Al}_x\text{Ga}_{1-x}\text{As}$  insulators on degenerate GaAs substrates. These inverted heterostructures are described in detail by Meirav, Kastner, and Wind;<sup>13</sup> the structure forms a metal-insulator-semiconductor field-effect transistor. Also described by these authors is the fabrication by electron-beam lithography of nanometer-sized gold electrodes that confine the electrons. Figure 1 is a sketch of

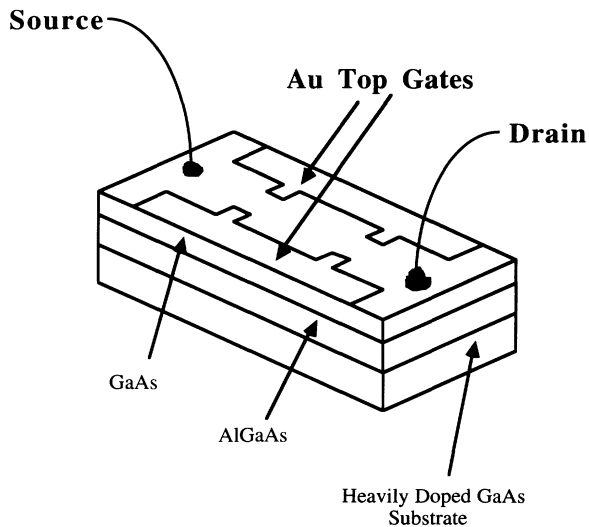


FIG. 1. Schematic diagram of the single-electron transistor used for the experiments reported here. The substrate, a crystal of heavily  $n$ -type GaAs, can be used as a gate. A layer of  $\text{Al}_x\text{Ga}_{1-x}\text{As}$  and a layer of pure GaAs are grown on the substrate, forming a metal-insulator-semiconductor field-effect transistor. A negative bias applied to the titanium-gold electrodes confines electrons in the GaAs to a narrow channel, and the protrusions create barriers through which electrons must tunnel. These gold electrodes were also used as a gate in the present measurements. The device studied here has about  $0.9 \mu\text{m}$  between the protrusions, and the width of the channel (except at the protrusions) is about  $0.5 \mu\text{m}$ .

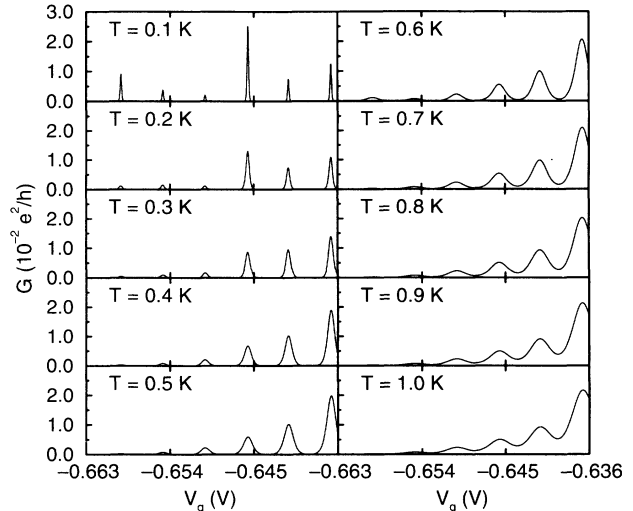


FIG. 2. Conductance as a function of voltage on the gold electrodes  $V_g$  for various temperatures. At low  $T$  the random variation of the peak height is evident, whereas at high  $T$  the general increase of conductance with  $V_g$  is apparent (see Fig. 3). The Coulomb blockade gap measured from the temperature dependence of the peak width is  $0.68 \text{ meV}$ . The spacing between the peaks is approximately  $4.5 \text{ mV}$ .

the device giving the electrode geometry. Ohmic contacts are made at each end of the narrow channel where the electrodes terminate, leaving a two-dimensional electron gas when a positive voltage is applied to the substrate. These are the source and drain for the transistor. A negative voltage is applied to the Ti-gold electrodes to confine the electrons to a small region between the two constrictions in the channel. These electrodes, like the substrate, can be used to vary the chemical potential of the electron gas. Indeed, in the following,  $V_g$  is the voltage applied to the Ti-gold electrodes.

Samples were bonded on nonmagnetic ceramic headers on the cold finger of a dilution refrigerator with a base temperature of  $25 \text{ mK}$ . The gold electrical leads are used to thermally lock the sample to wires thermally linked to the cold finger. As discussed by Meirav, Kastner, and

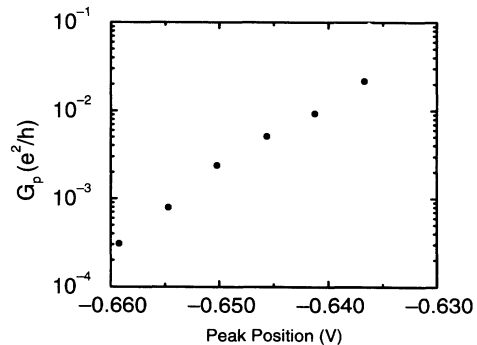


FIG. 3. The peak conductance as a function of peak position at  $1 \text{ K}$ , from the data of Fig. 2, on a logarithmic scale showing the exponential increase of the conductance. This is consistent with the idea that the conductance increases with  $V_g$  because the energy difference between the Fermi energy and the barrier decreases.

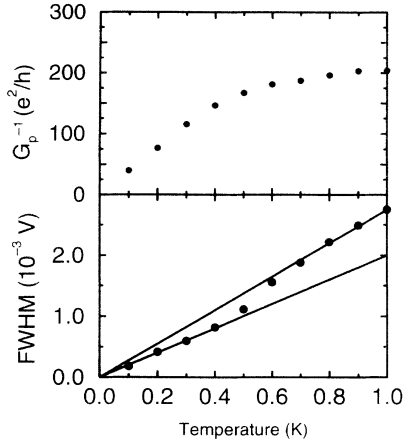


FIG. 4. The inverse of the peak conductance  $G_p^{-1}$  (upper panel) and the width of the peak (lower panel) as functions of temperature for the peak at  $V_g = -0.6455$  V in Fig. 2. This is the largest peak at 100 mK. The conductance varies as  $T^{-1}$  up to about 0.4 K. At the same temperature the slope of the linear increase of width with temperature changes from  $3.5kT$ , the value predicted for the single-level case (lower line), to  $4.35kT$  predicted for the multilevel case (upper line).

Wind,<sup>13</sup> the electron temperature as measured from the width of the conductance peaks follows the refrigerator temperature at high temperatures, but is warmer than the refrigerator at the lowest temperatures. We assume that this behavior is the result of heating of the electrons by electrical noise. We have minimized this source of heating by eliminating all digital electronics from the screened room surrounding the refrigerator and by substantial filtering. Nonetheless, for the present experiments, the lowest electron temperature obtainable was 100 mK. The peaks are independent of  $T$  below 100 mK, no data is shown for  $T < 100$  mK.

We have confirmed<sup>5</sup> that measurement of the intrinsic line shapes of conductance peaks requires application of

drain-source voltages  $V_{ds} < kT$ . Indeed, measurement of the increased width of the conductance peaks by either  $kT$  or  $eV_{ds}$  allows us to determine  $\alpha$  (see Ref. 5). Because we are concerned with the intrinsic peak shapes, all the measurements reported here were made with  $V_{ds} = 2 \mu\text{V}$ , corresponding to  $T = 25$  mK. All results reported in this paper are for measurements at zero magnetic field.

#### IV. RESULTS

A qualitative presentation of the temperature dependence of conductance peaks was given by Meirav, Kastner, and Wind.<sup>15</sup> Figure 2 shows the conductance as a function of gate voltage in more detail for temperatures between 100 mK and 1 K. Below 800 mK, where the peaks do not overlap, their shape is accurately described by Eqs. (3) or (5) as demonstrated by Foxman *et al.*<sup>5</sup>

The overall increase in conductance with increasing  $V_g$  results from the increased transmission of the barriers as  $V_g$  is increased; that is  $\Gamma_L$  and  $\Gamma_R$  increase exponentially with  $V_g$ . This is demonstrated in Fig. 3, where we plot the peak conductance as a function of  $V_g$  at the highest temperature on a logarithmic plot. The approximately exponential increase is consistent with lowering of the tunnel barrier. Foxman *et al.*<sup>5</sup> showed that the peak width (the larger of  $\Gamma_L$  and  $\Gamma_R$ ) also increases exponentially with  $V_g$ , as expected.

Next we examine the temperature dependence of individual conductance peaks. First consider the peak at  $-0.6455$  V, the largest peak in Fig. 2 at 100 mK. The upper panel of Fig. 4 shows the inverse of its amplitude as a function of  $T$ . The inverse amplitude is proportional to  $T$  at low  $T$  as predicted by the single-level form [Eq. (3)]. Above about 0.5 K the peak conductance becomes independent of temperature, as predicted by the multilevel form [Eqs. (4) or (5)].

The width of the peak also shows this crossover. The full width at half maximum is plotted as a function of  $T$  in the lower panel of Fig. 4. The shallower line in the lower panel is the single-level prediction,  $3.5kT$ , and the

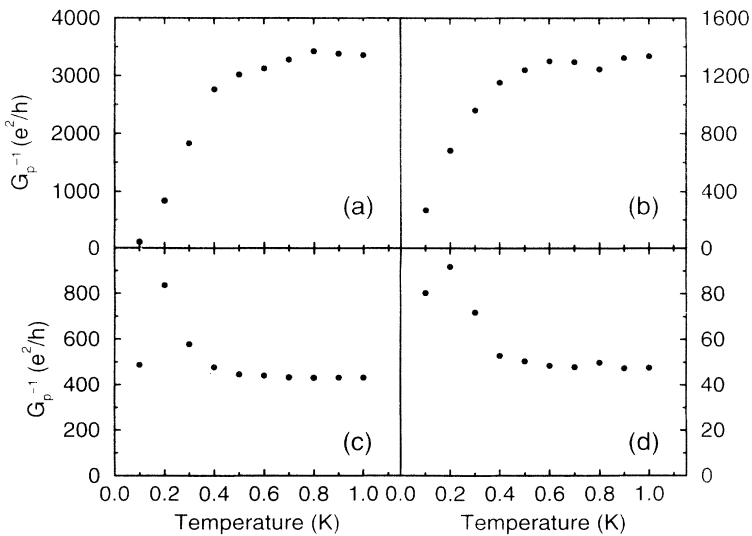


FIG. 5. Inverse of peak conductance for four other conductance peaks in Fig. 2. The gate voltage of the peaks is (a)  $-0.6593$  V, (b)  $-0.6548$  V, (c)  $-0.6503$  V, and (d)  $-0.6367$  V. The behavior in (b) is similar to that in Fig. 4, and is expected when a single level dominates the conductance at low  $T$ . The behavior in (c) and (d) results from the participation of two levels. However, the temperature dependence in (a) for the lowest gate-voltage peak in Fig. 2 is too strong to be compatible with current theoretical ideas.

steeper line is the multilevel prediction,  $4.35kT$ . This is dramatic evidence for the crossover from single-level to multilevel behavior, and shows that the crossover occurs in a narrow range of  $T$ . The crossover temperature is expected to be  $\sim \Delta E$ , which gives  $\Delta E \sim 40 \mu\text{eV}$ . This is consistent with level spacings measured by Foxman *et al.*<sup>5</sup> using source-drain tunneling spectroscopy.

Most of the peaks do not display this simple behavior, however. Figure 5 shows the inverse amplitude of all the other peaks in Fig. 2. All are temperature independent above  $\sim 0.5$  K, as expected for the multilevel regime. One other peak, that at  $V_g = -0.6548$  V [Fig. 5(b)], has the expected  $T^{-1}$  dependence, but the others do not.

Meir, Wingreen, and Lee<sup>10</sup> explained that peculiar temperature dependence of the peak heights is to be expected when there is a large variation of coupling strength,  $\Gamma_L \Gamma_R / \Gamma^2$ , from one peak to the next. Behavior like that for the peak at  $-0.6503$  V [Fig. 5(c)] is expected for a weakly coupled level adjacent to a strongly coupled one. When  $kT < \Delta E$  the conductance is dominated by the weakly coupled level, and its height, though small, is proportional to  $1/T$ . However, when  $kT$  approaches  $\Delta E$ , thermal excitation to the strongly coupled level causes the amplitude to increase with  $T$  until the multilevel regime is obtained. Less dramatic behavior of this kind can be seen as well for the peak at  $-0.6367$  V mV [Fig. 5(d)].

The lowest gate voltage conductance peak in Fig. 2 [Fig. 5(a)] cannot be described by the model presented here. Its height decreases with  $T$  much more rapidly than  $T^{-1}$ . We have no explanation for this behavior.

## V. DISCUSSION

The asymptotic behavior predicted by the single-level and multilevel expressions [Eqs. (3) and (4)] are seen in Figs. 4, 5(b), and 5(c). The amplitudes of the three peaks all decrease as  $T^{-1}$  at low  $T$ , and become independent of  $T$  at high  $T$ . However, the temperature dependence in the crossover regime depends on the coupling of individual levels to the leads. Consider a weakly coupled level.

At  $T=0$  the conductance is small and it decreases further as  $T$  is increased. However, if there is a strongly coupled level nearby in energy, it makes an additional contribution to the conductance that increases with  $T$ . Once  $kT$  is larger than the level spacing, however, the conductance becomes constant. Meir, Wingreen, and Lee<sup>10</sup> used the constant-interaction model successfully to describe the temperature dependencies of conductance peaks like those of Fig. 5. They assumed a  $\delta$ -function zero-temperature resonance line shape which gives a satisfactory approximation to the Lorentzian of Eq. (2) in the limit  $kT \gg \Gamma$ . To develop a little more intuition into how the peculiar temperature dependencies arise, we have evaluated the integral of Eq. (2) as a function of  $\mu$ . This gives the contribution to the conductance of a second level an energy  $\mu$  away from the resonant level. It may be helpful to think of this as the conductance one would measure if the resonant level had zero coupling and there was only one level nearby with finite coupling. The results are shown in Fig. 6, where  $\log_{10} G_s$  is plotted as a function of  $2\mu/\Gamma$  and  $\log_{10}(\Gamma/2kT)$ . At  $T$  low enough that  $\Gamma \gg kT$  the conductance follows the Lorentzian, as expected from Eq. (2). For high  $T$ ,  $G_s$  is independent of  $\mu$  because the width of the peak is  $3.5kT$  and for the range of  $\mu$  plotted,  $\mu \ll kT$ . In this high- $T$  regime, the conductance varies as  $T^{-1}$  because the derivative of the Fermi function has this dependence. On resonance,  $\mu=0$ , this  $T^{-1}$  behavior continues as  $T$  is decreased until  $kT \sim \Gamma$ . However, for nonzero  $\mu$  there is a maximum in  $G_s$  as a function of  $T$ .

Figure 7 displays these results in a different way. There  $\log_{10} G_s$  is plotted as a function of  $2\mu/\Gamma$  for different values of  $2kT/\Gamma$ . At  $T=0$  the conductance follows the Lorentzian form for all  $\mu$ . Increasing  $T$  from  $T=0$  at any fixed  $\mu \neq 0$ , the conductance will first increase with  $T$  for  $kT < \mu$  because of the thermally activated contribution of the coupled level. The roughly linear dependence of  $\log_{10} G_s$  on  $\mu$  for  $T=1.2\Gamma$  demonstrates this activated behavior clearly. However when  $kT \sim \mu$  the

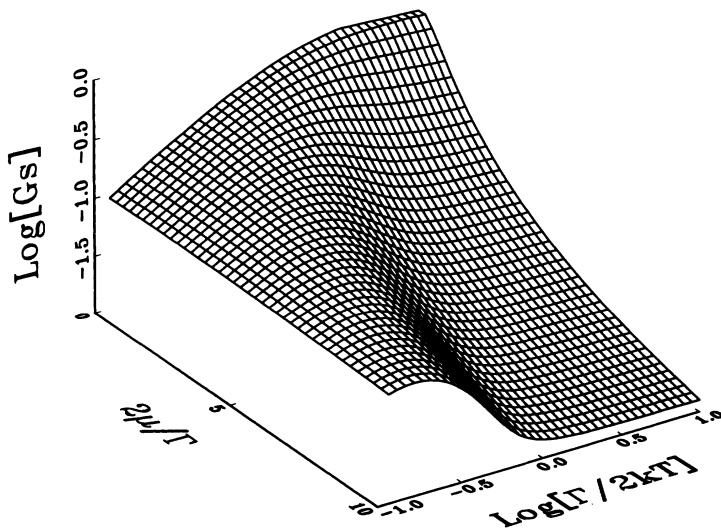


FIG. 6. Dependence of single-level conductance  $G_s$  on  $\mu$  and  $T$  from Eq. (2).  $\log_{10} G_s$  is plotted as a function of the dimensionless quantities  $2\mu/\Gamma$  and  $\log_{10}(\Gamma/2kT)$ . Note the peak in the  $T$  dependence for all  $\mu \neq 0$ .

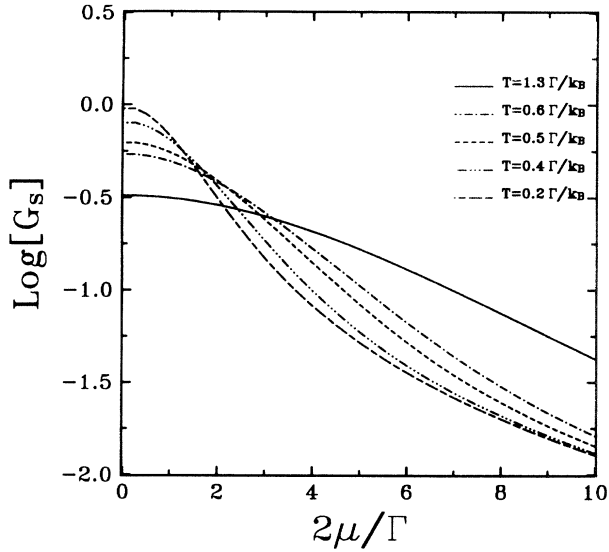


FIG. 7. Cuts through Fig. 6 at fixed  $\Gamma/kT$ . Note the linear dependence of  $\log_{10}G_s$  on  $T^{-1}$  for  $kT > \Gamma$  showing the activated conductance near a strongly coupled level.

width of the Fermi-Dirac peak becomes comparable to  $\mu$  and the dependence changes to the resonant one. On resonance the width increases linearly with  $T$  and the peak height decreases as  $T^{-1}$ . Thus at  $\mu \neq 0$  the peak height first increases with  $T$ , reaches a maximum, and then decreases again.

The qualitative behavior of peaks like those in Fig. 5 is

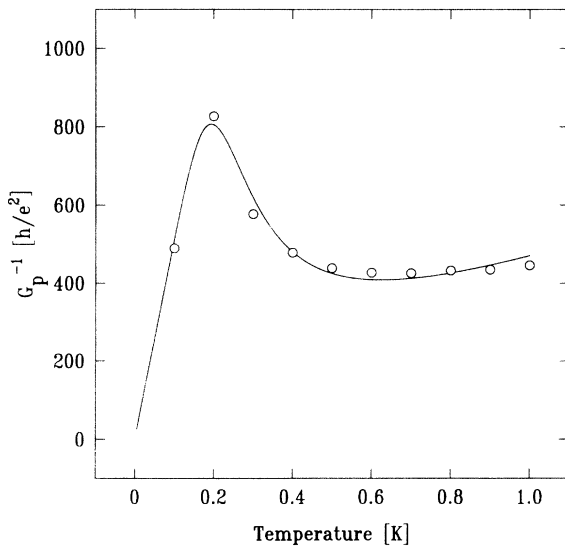


FIG. 8. Fit to the data for the peak at  $-0.6503$  V [Fig. 5(c)]. It is assumed that the conductance arises from a weakly coupled level with a more strongly coupled one nearby in energy. The only parameters are the energy separation and the relative coupling strengths of the two levels. The best fit gives an energy separation  $\Delta E = 45 \mu\text{eV}$ , and a coupling strength of the weakly coupled level 0.08 times that of the strongly coupled one. In particular, the fit is to the function  $G_p = A[Bf'(0) + f'(\Delta E)]$ , where  $f' = (4kT)^{-1} \text{sech}[\Delta E/2kT]$ , and the best fit gives  $A = 10^{-2} e^2/h$ ,  $B = 7.9 \times 10^{-2}$ , and  $\Delta E = 45 \text{meV}$ .

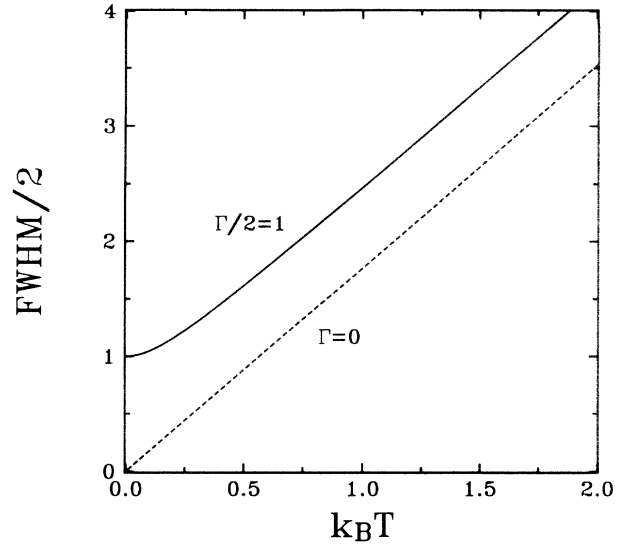


FIG. 9. Width as a function of temperature predicted by Eq. (2) compared with the result for  $\Gamma = 0$ .

thus easily understood. By adding a weakly coupled resonant level to a strongly coupled nonresonant one, the detailed  $T$  dependence can be fit quite well, as shown in Fig. 8 for the peak at  $V_g = -0.6503$  V in Fig. 2. The resonant level in this case has a coupling strength  $\frac{1}{10}$  that of its stronger neighbor. The maximum in the inverse amplitude occurs at the energy difference of the two levels, giving  $\Delta E \sim 40 \mu\text{eV}$  as before.

It is interesting to note, as shown in Fig. 9, that the underlying Lorentzian reveals itself at  $T \gg \Gamma$  as an excess width. The absence of such an offset in the data of Fig. 4 indicates that  $\Gamma \ll 10 \mu\text{eV}$  for the peak studied.

It is interesting to note that adjacent peaks in Fig. 2 have very different conductances and temperature dependences. One might have expected that the peaks would occur in pairs because of the spin degeneracy. That this does not happen shows that the state of the many-electron system changes completely every time an electron is added. This may be related to the low symmetry of the potential, which puts this system in the regime of quantum chaos.

Jalabert, Stone, and Alhssid<sup>7</sup> and Prigodin, Efetov, and Iida<sup>8</sup> have predicted the distribution function for the peak amplitudes at zero temperature. To test these predictions one must measure a large number of peaks whose amplitudes vary as  $T^{-1}$ . Those whose amplitudes increase with  $T$  are associated with resonances so weakly coupled that their amplitude is dominated by a well-coupled neighboring level. Since the theories predict that the distribution function is maximum near zero coupling, only the high-coupling tail of the distribution can be measured. Measurements of this kind are now in progress. Of course, a theory which predicted the measured distribution function including the  $T$  dependence could readily be tested. Furthermore, other features predicted by the theories of quantum chaos are not so sensitive to weakly coupled levels and can be tested with artificial atoms.

The measurements reported here show clearly the

crossover from single-level to multilevel conductance in an artificial atom. It is clear that one can reach the single-level regime for large conductance resonances. However, one must ascertain that the conductance varies as  $T^{-1}$  in order to be sure that the conductance of a weakly coupled level is not overestimated because of an adjacent strongly coupled one.

#### ACKNOWLEDGMENTS

We are grateful to N. S. Wingreen and Y. Meir for helpful discussions. This work was supported by NSF Grant No. ECS 9203427, and by the U.S. Joint Services Electronics Program under Contract No. DAALL03-93-C-0001.

<sup>1</sup>M. A. Kastner, *Phys. Today* **46** (1), 24 (1993).

<sup>2</sup>D. J. Thouless, *Phys. Rev. Lett.* **39**, 1167 (1977).

<sup>3</sup>For a review, see D. V. Averin and K. K. Likharev, in *Mesoscopic Phenomena in Solids*, edited by B. Altshuler, P. A. Lee, and R. A. Webb (Elsevier, Amsterdam, 1990).

<sup>4</sup>P. L. McEuen, E. B. Foxman, J. Kinaret, U. Meirav, M. A. Kastner, N. S. Wingreen, and S. J. Wind, *Phys. Rev. B* **45**, 11 419 (1992).

<sup>5</sup>E. B. Foxman, P. L. McEuen, U. Meirav, N. S. Wingreen, Y. Meir, P. A. Belk, N. R. Belk, and M. A. Kastner, *Phys. Rev. B* **47**, 10 020 (1993).

<sup>6</sup>A. T. Johnson, L. P. Kouwenhoven, W. de Jong, N. C. van der Vaart, C. J. P. M. Harmans, and C. T. Foxon, *Phys. Rev. Lett.* **69**, 1592 (1992).

<sup>7</sup>R. A. Jalabert, A. D. Stone, and Y. Alhssid, *Phys. Rev. Lett.* **68**, 3468 (1992).

<sup>8</sup>V. N. Prigodin, K. B. Efetov, and S. Iida, *Phys. Rev. Lett.* **71**, 1230 (1993).

<sup>9</sup>B. D. Simons and B. L. Altshuler, *Phys. Rev. B* **48**, 5422 (1993).

<sup>10</sup>Y. Meir, N. S. Wingreen, and P. A. Lee, *Phys. Rev. Lett.* **66**, 3048 (1991).

<sup>11</sup>C. W. J. Beenakker, *Phys. Rev. B* **44**, 1646 (1991).

<sup>12</sup>D. V. Averin and A. N. Korotkov, *Zh. Eksp. Teor. Fiz.* **97**, 1661 (1990) [*Sov. Phys. JETP* **70**, 937 (1990)].

<sup>13</sup>U. Meirav, M. A. Kastner, and S. J. Wind, *Phys. Rev. Lett.* **65**, 771 (1990).

<sup>14</sup>I. O. Kulik, and R. I. Shekhter, *Zh. Eksp. Teor. Fiz.* **68**, 623 (1975) [*Sov. Phys. JETP* **41**, 308 (1975)].

<sup>15</sup>U. Meirav, P. L. McEuen, M. A. Kastner, E. B. Foxman, A. Kumar, and S. J. Wind, *Z. Phys. B* **85**, 357 (1991).